

NJC

Accepted Manuscript



This is an *Accepted Manuscript*, which has been through the Royal Society of Chemistry peer review process and has been accepted for publication.

Accepted Manuscripts are published online shortly after acceptance, before technical editing, formatting and proof reading. Using this free service, authors can make their results available to the community, in citable form, before we publish the edited article. We will replace this *Accepted Manuscript* with the edited and formatted *Advance Article* as soon as it is available.

You can find more information about *Accepted Manuscripts* in the [Information for Authors](#).

Please note that technical editing may introduce minor changes to the text and/or graphics, which may alter content. The journal's standard [Terms & Conditions](#) and the [Ethical guidelines](#) still apply. In no event shall the Royal Society of Chemistry be held responsible for any errors or omissions in this *Accepted Manuscript* or any consequences arising from the use of any information it contains.



Journal Name

ARTICLE

Alkyl groups-directed assembly of coordination polymers based on bis-(4-imidazol-1-yl-phenyl)-amine and their photocatalytic properties

Received 00th January 20xx,
Accepted 00th January 20xx

DOI: 10.1039/x0xx00000x

www.rsc.org/

Hong-Jian Cheng*, Ya-Li Shen, Yi-Feng Lu, Ji Ma, Hong-Wei Ji, Wen-Yu Yin, Xiao-Yan Tang, Yun-Sheng Ma and Rong-Xin Yuan*

Hydrothermal reactions of $\text{Zn}(\text{NO}_3)_2 \cdot 6\text{H}_2\text{O}$ or $\text{CdCl}_2 \cdot 2.5\text{H}_2\text{O}$ with bis-(4-imidazol-1-yl-phenyl)-amine (bimpa) and 5-methyl-1,3-benzenedicarboxylic acid (5-Me-1,3-H₂BDC) or 5-tert-butyl-1,3-benzenedicarboxylic acid (5-tb-1,3-H₂BDC) afforded four coordination polymers, $[\text{Zn}_2(5\text{-Me-1,3-BDC})_2(\text{bimpa})_2]_n$ (**1**), $\{[\text{Cd}_2(5\text{-Me-1,3-BDC})_2(\text{bimpa})(\text{H}_2\text{O})_4] \cdot \text{H}_2\text{O}\}_n$ (**2**), $\{[\text{Zn}(5\text{-tb-1,3-BDC})(\text{bimpa})] \cdot 2\text{H}_2\text{O}\}_n$ (**3**) and $\{[\text{Cd}(5\text{-tb-1,3-BDC})(\text{bimpa})] \cdot \text{H}_2\text{O}\}_n$ (**4**). Complexes **1-4** were characterized by elemental analysis, IR, powder X-ray diffraction, and single-crystal X-ray diffraction. **1** exhibits a 4-fold interpenetrating 3D framework in which 1D curvilinear chains are interconnected by bipma ligands. **2** can be considered as a 3D supramolecular architecture based on 2D entanglements which are consisted of 1D tubes in parallel interpenetration. **3** and **4** respectively have 2D (6⁵-8) layers (**3**) and 2D layers constructed by 1D tubes (**4**), which are further extended into two 3D supramolecular architecture through weak hydrogen-bonding and π - π interactions. The solid state luminescent and optical properties of **1-4** at ambient temperature were also investigated. A comparative study on their photocatalytic activity toward the degradation of methylene blue in polluted water was explored.

Introduction

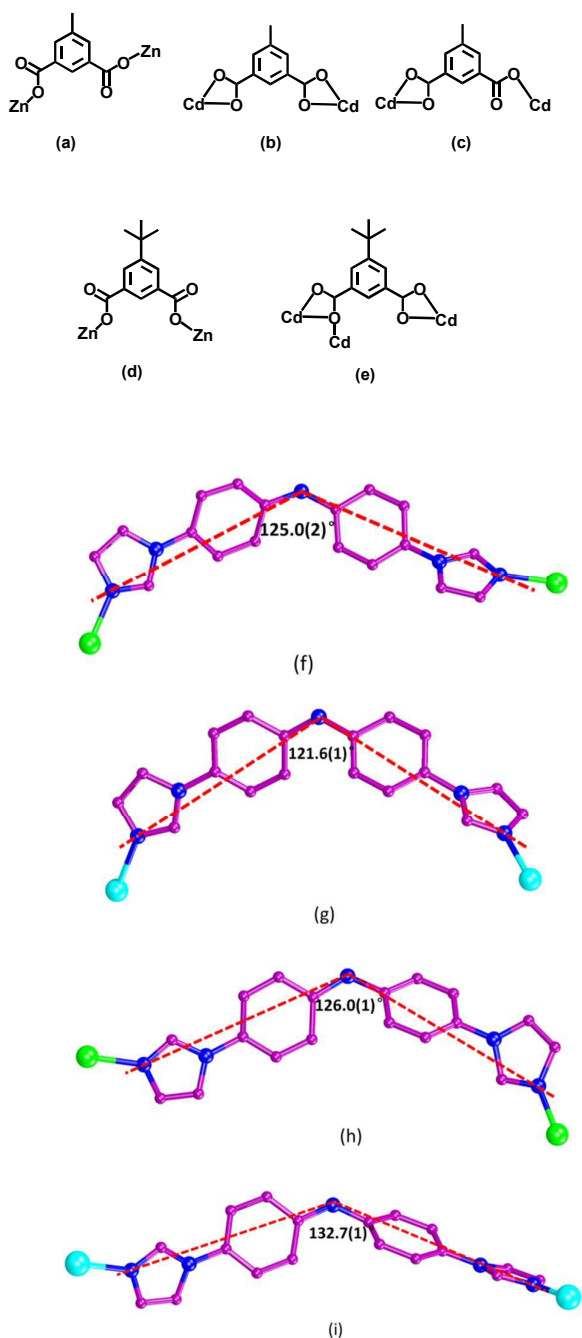
Over the past decade years, the study of various coordination polymers (CPs) displaying intriguing architectures¹ or potential applications in absorption,² separation,³ magnetism,⁴ luminescence,⁵ catalysis,⁶ have received considerable attention. Although plenty of CPs have been reported, it is still a huge challenge to synthesize the expected structures influenced by several factors, including organic ligands, metal centres, ratio of reactants, solvents, reaction temperatures and pH values.⁷ On the other hand, these uncertainties also provide us suitable strategies to systematically study the relationship between the above factors and the resulting frameworks.⁸ Among them, the geometry or substituted groups of organic ligands as well as the coordination geometry of metal centres are especially important in the assembly of novel motifs.⁹ For instance, solvothermal reactions of $\text{Zn}(\text{OAc}) \cdot 2\text{H}_2\text{O}$ or $\text{Cd}(\text{OAc}) \cdot 2\text{H}_2\text{O}$ with 5-Me-1,3-H₂BDC or 5-tb-1,3-H₂BDC and 1,3-bis(4-pyridyl)propane (bpp) produced 4-fold interpenetrated diamondoid-like networks $[\text{Zn}(5\text{-Me-1,3-BDC})(\text{bpp})]_n$ or $[\text{Cd}(5\text{-Me-1,3-BDC})(\text{bpp})]_n$, 2D corrugated networks $\{[\text{Zn}(5\text{-tb-1,3-BDC})(\text{bpp})] \cdot 2\text{H}_2\text{O}\}_n$ and 3D supramolecular networks

$\{[\text{Cd}(5\text{-tb-1,3-BDC})(\text{bpp})(\text{H}_2\text{O})] \cdot 3\text{H}_2\text{O}\}_n$.¹⁰ The employment of introducing alkyl groups into backbond of organic ligands can modify the resulting frameworks and improve their properties such as water stability and flexibility, which is of paramount importance for a wide range of applications.¹¹

Recently, we have paid attention to a type of bi-imidazolyl ligands based on rigid and linear diphenyl, such as 4,4'-bis(1-imidazolyl)biphenylene,¹² 4,4'-bis(benzoimidazol-1-yl)biphenylene,¹³ 2-amine-4,4'-bis(1-imidazolyl)-biphenylene,¹⁴ which were used to reaction with carboxylic acids and metal ions to afford several novel CPs. If we introduce a bent bi-imidazolyl ligand, can the resulting ligand in the assembly procedure produce different topological structures and properties compared with the above ligands? With this in mind, under microwave-assisted solvent- and ligand-free conditions¹⁵ we synthesized a novel bi-imidazolyl ligand, bis-(4-imidazol-1-yl-phenyl)-amine (bimpa) (Scheme 1), which belongs to curved ligand and that is an unexplored ligand for forming CPs. In this work, we have selected two 5-R-1,3-benzenedicarboxylic acid derivatives (R = Me, tert-butyl) and bipma (Scheme 1), to react with $\text{Zn}(\text{NO}_3)_2 \cdot 6\text{H}_2\text{O}$ or $\text{CdCl}_2 \cdot 2.5\text{H}_2\text{O}$ under the hydrothermal conditions. Four different coordination polymers, $[\text{Zn}_2(5\text{-Me-1,3-BDC})_2(\text{bimpa})_2]_n$ (**1**), $\{[\text{Cd}_2(5\text{-Me-1,3-BDC})_2(\text{bimpa})(\text{H}_2\text{O})_4] \cdot \text{H}_2\text{O}\}_n$ (**2**), $\{[\text{Zn}(5\text{-tb-1,3-BDC})(\text{bimpa})] \cdot 2\text{H}_2\text{O}\}_n$ (**3**) and $\{[\text{Cd}(5\text{-tb-1,3-BDC})(\text{bimpa})] \cdot \text{H}_2\text{O}\}_n$ (**4**) were isolated. Herein, we report their syntheses, crystal structures, luminescent, and optical and photocatalytic performances.

School of Chemistry and Materials Engineering, Jiangsu Key Laboratory of Advanced Functional Materials, Changshu Institute of Technology, Changshu, Jiangsu, 215500, P. R. China. Fax: 86-512-52251842; E-mail: hjcheng@cslq.cn (H. -J. Cheng); yuanrx@cslq.edu.cn (R. -X. Yuan).

† Electronic supplementary information (ESI) available: CCDC reference numbers 1423960~1423963 for **1-4**. For ESI and crystallographic data in CIF or other electronic format see DOI: 10.1039/xxxxxxx



Scheme 1 The coordination modes of 5-Me-1,3-BDC in **1** (a), 5-Me-1,3-BDC in **2** (b or c), 5-tb-1,3-BDC in **3** (d), 5-tb-1,3-BDC in **4** (e), bimpa in **1** (f), bimpa in **2** (g), bimpa in **3** (h) and bimpa in **4** (i).

Experimental

Materials and methods

The bis(4-bromophenyl)amine was prepared according to the literature method.¹⁶ Other chemicals and reagents were obtained from commercial sources and used as received. Elemental analyses for C, H and N were performed on a

PE2400 elemental analyzer. The FT-IR spectra were recorded on a Nicolet 380 spectrometer with pressed KBr pellets (4000–400 cm^{-1}). The powder X-ray diffraction (PXRD) measurements were carried out on a Rigaku D/max-2200/PC system. The fluorescent spectra were recorded on a Hitach F-4600 fluorescence spectrometer with polycrystalline sample. UV-vis diffusion reflectance absorption spectra were recorded with a Shimadzu UV-3600 spectrophotometer, where an integrating sphere was used in diffusion reflectance absorption analysis. Single crystal X-ray diffraction was carried out with a Bruker Smart Apex II CCD diffractometer for **1**, **2** and **3**, Rigaku Mercury CCD X-ray diffractometer for **4**.

Preparation of compounds bimpa and 1–4

bimpa. A 10 mL deep porcelain crucible was filled with a mixture of 1.635 g (5.0 mmol) bis(4-bromophenyl)amine, 3.404 g (50.0 mmol) imidazole, 2.073 g (15.0 mmol) anhydrous potassium carbonate and 0.190 g (1.0 mmol) cuprous iodide. The reaction mixture was exposed to microwave irradiation at different temperatures and times. After cooling to room temperature, the residue was diluted with 20 mL H_2O . 0.146 g (0.5 mmol) ethylenediaminetetraacetic acid and 2 mL $\text{NH}_3 \cdot \text{H}_2\text{O}$ (28–29%) was added, and the resulting mixture was stirred at room temperature for 24 h. The resulting dark brown precipitate was filtered and further purified by recrystallization in methanol to form gray needles of bimpa. Yield: 1.16 g (77 %). m.p. 216.8–217.2 °C. Anal. Calcd for $\text{C}_{18}\text{H}_{15}\text{N}_5$: C 71.74; H 5.02; N 23.24; found C 71.54; H 5.32; N 23.34. IR (KBr, cm^{-1}): 3219(m), 3110(m), 1601(m), 1522(s), 1394(w), 1311(m), 1056(s), 827(m), 741(m), 624(m). ^1H NMR ($\text{DMSO}-d_6$, 400 MHz, ppm) δ 8.54 (s, 1H), 8.16 (s, 2H), 7.66 (s, 2H), 7.51 (d, $J = 8.4$ Hz, 4H), 7.19 (d, $J = 8.4$ Hz, 4H), 7.11 (s, 2H).

[Zn₂(5-Me-1,3-BDC)₂(bimpa)₂]_n (1**)**. To a 10 mL Pyrex glass tube was added $\text{Zn}(\text{NO}_3)_2 \cdot 6\text{H}_2\text{O}$ (23 mg, 0.1 mmol), 5-Me-1,3- H_2BDC (18 mg, 0.1 mmol), bimpa (30 mg, 0.1 mmol), H_2O (2 mL) and MeCN (0.5 mL). The tube was sealed and heated in an oven to 150 °C for 1 d and then cooled to ambient temperature at the rate of 5 °C h^{-1} to form brown blocks of **1**, which were washed with water–methanol and dried in air. Yield: 23 mg (43% yield based on Zn). Anal. Calcd. for $\text{C}_{54}\text{H}_{42}\text{Zn}_2\text{N}_{10}\text{O}_8$: C 59.52; H 3.88; N 12.85. Found: C 59.38; H 3.76; N 12.93. IR (KBr, cm^{-1}): 3364(w), 3117(w), 2933(vw), 1623(s), 1576(s), 1522(s), 1336(m), 1077(m), 824(m), 777(m), 729(m), 647(m), 511(w).

[Cd₂(5-Me-1,3-BDC)₂(bimpa)(H₂O)₄·H₂O]_n (2**)**. Complex **2** was prepared using a procedure similar to that adopted for **1** using $\text{CdCl}_2 \cdot 2.5\text{H}_2\text{O}$ (24 mg, 0.1 mmol) in place of $\text{Zn}(\text{NO}_3)_2 \cdot 6\text{H}_2\text{O}$. Yield: 22 mg (45% yield based on Cd). Anal. Calcd. for $\text{C}_{36}\text{H}_{37}\text{Cd}_2\text{N}_5\text{O}_{13}$: C 44.46; H 3.83; N 7.20. Found: C 44.33; H 3.66; N 7.43. IR (KBr, cm^{-1}): 3432(w), 3247(m), 3138(w), 1644(s), 1610(s), 1569(s), 1514(s), 1343(s), 1241(m), 1118(m), 1063(m), 804(m), 770(m), 736(m), 647(m).

{[Zn(5-tb-1,3-BDC)(bimpa)]·2H₂O}_n (3**)**. Complex **3** was prepared using a procedure similar to that adopted for **1** using 5-tb-1,3- H_2BDC (22 mg, 0.1 mmol) in place of 5-Me-1,3- H_2BDC . Yield: 45 mg (72% yield based on Zn). Anal. Calcd. for

$C_{30}H_{31}ZnN_5O_6$: C 57.84; H 5.02; N 11.24. Found: C 57.63; H 4.86; N 11.40. IR (KBr, cm^{-1}): 3432(w), 3350(w), 3131(w), 1610(s), 1528(s), 1364(s), 1063(s), 824(m), 722(w), 654(w).

{[Cd(5-tb-1,3-BDC)(bimpa)]·H₂O}_n (4). Complex **4** was prepared using a procedure similar to that adopted for **3** using $CdCl_2 \cdot 2.5H_2O$ (24 mg, 0.1 mmol) in place of $Zn(NO_3)_2 \cdot 6H_2O$. Yield: 24 mg (37% yield based on Cd). Anal. Calcd. for $C_{30}H_{29}CdN_5O_5$: C 55.26; H 4.48; N 10.74. Found: C 55.43; H 4.56; N 10.60. IR (KBr, cm^{-1}): 3432(m), 3131(m), 1610(m), 1562(s), 1521(s), 1405(s), 1125(w), 1063(m), 831(w), 729(m), 647(m), 531(m).

X-ray Crystallography

Single crystals of **1-4** suitable for X-ray analysis were obtained directly from the above preparations. All measurements were made on a Bruker SMART APEX II (**1**, **2** and **3**) or Rigaku Mercury (**4**) CCD X-ray diffractometer using graphite monochromated Mo-K α ($\lambda = 0.71073 \text{ \AA}$). Cell parameters were refined on all observed reflections using the program *Crystalclear* (Rigaku and MSc, Ver. 1.3, 2001). The collected data were reduced by the program *CrystalClear*, and an absorption correction (multi-scan) was applied. The reflection data were also corrected for Lorentz and polarization effects.

The crystal structures of **1-4** were solved by direct methods and refined on F^2 by full-matrix least-squares methods with the *SHELXL-2014* program.¹⁷ In **3**, the N3, C5, C6, C7, C10, C11, C12, C13, C17 and C18 atoms of one bipma ligand and the C30 atoms of one 5-tb-1,3-BDC ligands are disordered over two sites with an occupancy factor of 0.53/0.47 for N3/N3A, C5/C5A, C6/C6A, C7/C7A, C10/C10A, C11/C11A, C12/C12A, C13/C13A, C17/C17A, C18/C18A and C30/C30A. In **4**, the C28, C29 and C30 atoms of one 5-tb-1,3-BDC ligands are disordered over

two sites with an occupancy factor of 0.32/0.68 for C28/C28A, C29/C29A and C30/C30A.

All of the non-H atoms were refined anisotropically. The H atoms of the water molecule in **2**, **3** and **4** were located from the Fourier map. All other H atoms were placed in geometrically idealized positions (C-H = 0.96 \AA for methyl groups, N-H = 0.86 \AA for amino groups, O-H = 0.82 \AA for hydroxyl groups, or C-H = 0.93 \AA for phenyl groups) and constrained to ride on their parent atoms with $U_{iso}(H) = 1.5U_{eq}(C)$ for methyl groups, $1.2U_{eq}(N)$ for amino groups, and $1.5U_{eq}(O)$ for hydroxyl groups. All the calculations were performed on a Dell workstation using the *CrystalStructure* crystallographic software package (Rigaku and MSC, Ver.3.60, 2004). A summary of the important crystallographic information for **1-4** are summarized in Table 1.

Photocatalytic activity study

The photocatalytic activities of the solid samples **1-4** were evaluated by the degradation of MB in aqueous solution. 80 mL of a methylene blue (MB) aqueous solution with a concentration of 0.032 $g L^{-1}$ were mixed with 40 mg of the catalysts, respectively. The suspensions were firstly stirred in the dark for about 3 h to guarantee the establishment of a sorption/desorption equilibrium. A 300 W high pressure mercury vapor lamp with circulating water cooling system was used as the UV resource at 10 cm distance between the liquid surface and the lamp. During the degradation, the mixture was stirred continuously with a magnetic stirrer. At regular time intervals, a 2 mL solution was sampled, centrifuged and filtered. The degradation progress was monitored by observing the intensity of the characteristic absorption band of MB at 663 nm. The UV-Vis absorption spectra of MB aqueous solutions were measured using an Agilent Cary-300 spectrophotometer.

Table 1 Summary of crystal data and structure refinement parameters for **1-4**

	1	2	3	4
Empirical formula	$C_{54}H_{42}Zn_2N_{10}O_8$	$C_{36}H_{37}Cd_2N_5O_{13}$	$C_{30}H_{31}ZnN_5O_6$	$C_{30}H_{29}CdN_5O_5$
Formula mass	1089.76	972.50	622.99	651.99
Crystal system	Orthorhombic	Monoclinic	Monoclinic	monoclinic
Space group	$P2_12_12_1$	$P2_1/n$	$P2_1/c$	$P2_1/c$
Crystal dimension (mm^3)	$0.3 \times 0.3 \times 0.2$	$0.2 \times 0.2 \times 0.2$	$0.4 \times 0.2 \times 0.2$	$0.3 \times 0.20 \times 0.2$
$a/\text{\AA}$	11.616(4)	16.404(4)	12.022(1)	10.209(2)
$b/\text{\AA}$	14.825(4)	11.977(3)	11.430(1)	17.349(3)
$c/\text{\AA}$	36.389(11)	20.202(5)	23.959(2)	17.192(3)
$\beta/^\circ$	90	94.188(5)	116.820(3) ^e	96.73(3) ^e
$V/\text{\AA}^3$	4998(3)	3958.5(15)	2938.1(3)	3024(1)
$D_c/g\text{ cm}^{-3}$	1.448	1.632	1.408	1.432
Z	4	4	4	4
μ (Mo-K α)/ mm^{-1}	1.026	1.144	0.887	0.768
$F(000)$	2240	1952	1296	1328
Total reflections	42412	26009	24173	30721
Unique reflections	8629	6636	6620	6915
No observations	7713	5356	4896	5338
No parameters	668	505	497	398
R_1^a	0.0562	0.0367	0.0698	0.0511
wR_2^b	0.1508	0.1430	0.1415	0.1239
GOF ^c	1.09473	1.074	1.043	1.084
$\Delta\rho_{max}/\Delta\rho_{min}$ ($e\text{-\AA}^{-3}$)	1.065, -0.798	0.826, -1.070	0.535, -0.466	0.824, -0.535

^a $R_1 = \sum ||F_o| - |F_c|| / \sum |F_o|$. ^b $wR_2 = \{\sum w(F_o^2 - F_c^2)^2 / \sum w(F_o^2)^2\}^{1/2}$. ^c $GOF = \{\sum w(F_o^2 - F_c^2)^2 / (n - p)\}^{1/2}$, where n = number of reflections and p = total numbers of parameters refine

Journal Name

ARTICLE

Results and discussion

Synthetic and spectral aspects

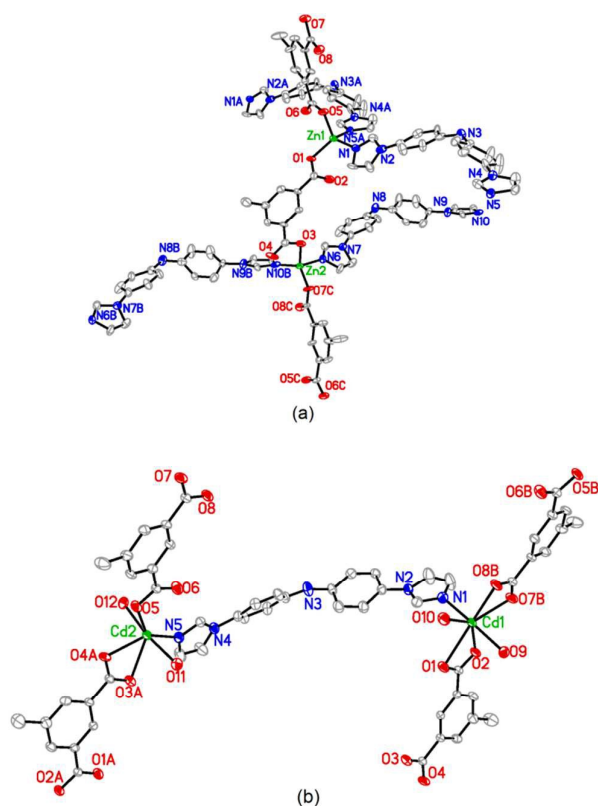
The hydrothermal reactions of bimpa and 5-Me-1,3-H₂BDC or 5-tb-1,3-H₂BDC with Zn(NO₃)₂·6H₂O in a 1 : 1 : 1 molar ratio at 150 °C in a sealed Pyrex glass for one day gave rise to brown block crystals of **1** (43% yield based on Zn) and **3** (72% yield based on Zn). To study the influence of the metals on their complex structures, analogous reactions with CdCl₂·2.5H₂O afforded brown block crystals of **2** (43 %), and **4** (37% yield). Complexes **1-4** are air- and moisture-stable, and insoluble in common solvents such as water, toluene, benzene, acetonitrile, methanol, acetone, DMF and DMSO. The elemental analyses were consistent with their chemical formulas. Powder X-ray diffraction (PXRD) was employed to confirm the bulk phase homogeneity of the four complexes. The measured PXRD patterns of **1-4** were closely matched with the simulated patterns generated from the results of single crystal X-ray diffraction data (Fig. S1). The identities of **1-4** were further confirmed by single crystal X-ray diffraction analysis.

Crystal structures of **1-4**

Being crystallized in the orthorhombic space group $P2_12_12_1$ (**1**), monoclinic space groups $P2_1/n$ (**2**), $P2_1/c$ (**3**) and $P2_1/c$ (**4**), the asymmetric units for **1-4** consist of one [Zn₂(5-Me-1,3-BDC)₂(bimpa)₂] molecule (**1**), one [Cd₂(5-Me-1,3-BDC)₂(bimpa)(H₂O)₄] molecule and one water solvent molecules (**2**), a [Zn(5-tb-1,3-BDC)(bimpa)] molecule and two water solvent molecules (**3**), or [Cd(5-tb-1,3-BDC)(bimpa)] molecule and a water solvent molecule (**4**), respectively. In **1** or **3**, each Zn atom has a tetrahedral coordination geometry, coordinated by two O atoms from two 5-Me-1,3-BDC or 5-tb-1,3-BDC ligands and two N atoms from two bimpa ligands (Fig. 1a and 1c). The mean Zn-N and Zn-O bond lengths (2.020(11) Å vs 1.968(7) Å) (**1**) or (1.988(2) Å vs 1.948(2) Å) (**3**) are in the normal range and similar to those of the corresponding ones of [Zn(1,3-BDC)(bmimb)]_n (2.040(3) Å vs. 1.972(5) Å; bmimb = 4,4'-bis(4-methyl-1-imidazolyl)biphenylene).¹⁸ In **2**, Cd1 adopts a pentagonal bipyramidal geometry, coordinated by four O atoms from two bimpa ligands, two O atoms from different H₂O molecules and one N atom from a bimpa ligand, while Cd2 is octahedrally coordinated by three O atoms from two 5-Me-1,3-BDC ligands, two O atoms from different H₂O molecules and one N atom from a bimpa ligand (Fig. 1b). For **4**, each Cd1 atom is seven-coordinated by five O atoms from three 5-tb-1,3-BDC ligands and two N atoms from two bimpa ligands (Fig. 1d). The average Cd-N and Cd-O bond lengths (2.257(4) Å vs 2.387(3) Å) (**2**) or (2.323(4) Å vs 2.447(3) Å) (**4**) are comparable

to those found in the Cd-based CPs such as [Cd(5-Me-1,3-BDC)(bimb)] (2.312(1) Å or 2.340(3) Å, bimb = 4,4'-bis(1-imidazolyl)biphenylene).¹²

In complexes **1-4**, four carboxylate ligands display different coordination modes shown in Scheme 1. For **1** and **3**, each deprotonated carboxylate group of 5-Me-1,3-BDC or 5-tb-1,3-BDC ligand acts as a monodentate coordination mode (Scheme 1a and 1d). In **2**, 5-Me-1,3-BDC ligands adopt two coordination modes: bis-chelating ones and monodentate/chelating ones (Scheme 1b or 1c). In **4**, 5-tb-1,3-BDC adopts a bridging-chelating/chelating coordination mode (Scheme 1e). Each bimpa in **1-4** adopts slightly different conformations with the angles (N1-N3-N5) (125.0(2)° or 124.9(2)° (**1**), 121.6(1)° (**2**), 126.0(1)° (**3**) and 132.7(1)° (**4**) (Scheme 1f-i).



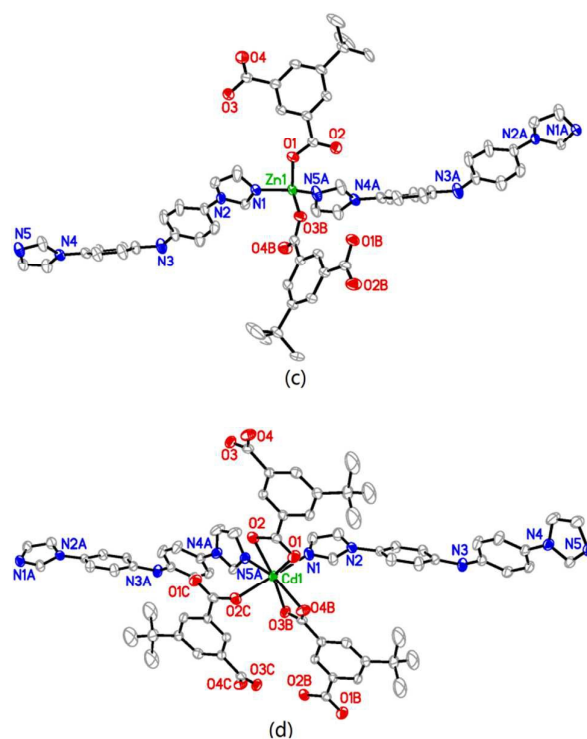


Fig. 1 (a) View of the coordination environment of Zn in **1** with a labeling scheme and 30% thermal ellipsoids. Symmetry codes: (A) $x + 1, y + 1, z$; (B) $x + 1, y - 1, z$; (C) $-x + 1/2, -y, z + 1/2$. (b) View of the coordination environment of Zn in **2** with a labeling scheme and 30% thermal ellipsoids. Symmetry codes: (A) $-x + 3, -y + 1, -z + 2$; (B) $-x + 2, -y, -z + 2$; (c) View of the coordination environment of Zn in **3** with a labeling scheme and 30% thermal ellipsoids. Symmetry codes: (A) $x - 1, y + 1, z$; (B) $-x + 1, y + 1/2, -z + 3/2$. (d) View of the coordination environment of Zn in **4** with a labeling scheme and 30% thermal ellipsoids. Symmetry codes: (A) $x, y + 1, z$; (B) $-x + 1, -y + 1, -z + 1$; (C) $x - 1, y, z$.

In **1-4**, metal ions are bridged by 5-Me-1,3-BDC or 5-tb-1,3-BDC ligands to form a 1D curvilinear chain [Zn(5-Me-1,3-BDC)] (the neighboring Zn...Zn distance of 9.532(3) Å) (**1**) (Fig. 2a), 1D linear chain [Cd(5-Me-1,3-BDC)] (the neighboring Cd1...Cd2 distance of 10.312(2) Å) (**2**) (Fig. 2b), 1D helix chain [Zn(5-tb-1,3-BDC)] (the neighboring Zn...Zn distance of 7.935(1) Å) (**3**) (Fig. 2c) and 1D ribbon based on binuclear [Cd₂(COO)₄] unit (the Cd...Cd distance of 3.846(1) Å and Cd-O-Cd angle of 100.24(13)°) (**4**) (Fig. 2d).

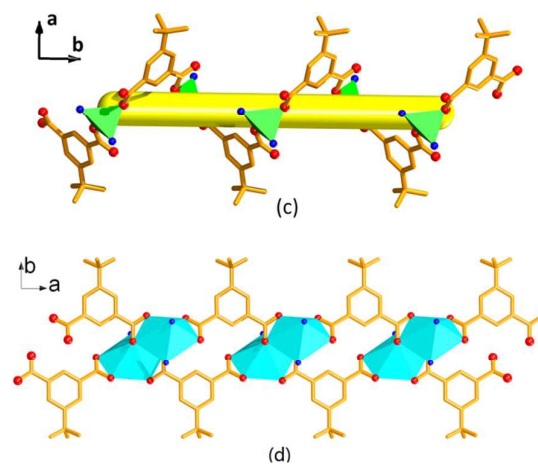
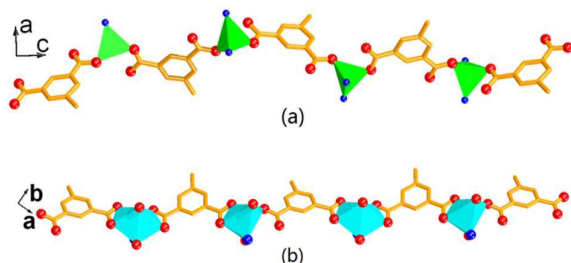
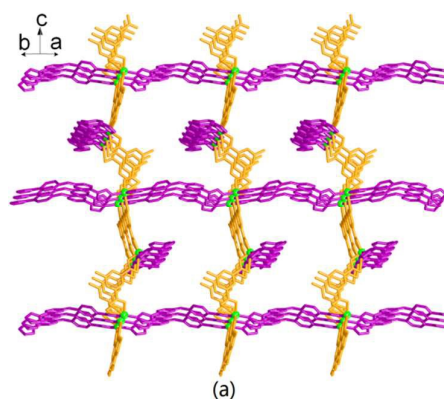


Fig. 2 (a) View of the 1D curvilinear chain in **1** extending along the c axis. (b) View of the 1D linear chain in **2**. (c) View of 1D helix chain in **3** extending along the b axis. (d) View of the 1D ribbon in **4** along the a axis. Each green and cyan polyhedrons represent one Zn and Cd atom, respectively. The red and blue balls represent O and N atom, respectively.

These 1D units are extended through *bimpa* into different frameworks. For **1**, each chain is further connected to its four equivalent ones *via bimpa* ligands to form a 3D framework (Fig. 3a). Such a single 3D framework has 1D channels ($ca. 20.88 \text{ \AA} \times 17.11 \text{ \AA}$) along the a axis. Topologically, such a 3D net can be regarded as having a uninodal 4-connected topological structure with a $(6^5 \cdot 8)$ Schläfli symbol (Fig. 3b), in which each Zn acts as a 4-connecting node. Although the single net of **1** has large channels, its void space is filled by mutual interpenetration of three independent equivalent nets, generating a four-fold interpenetrating 3D architecture (Fig. 3c).



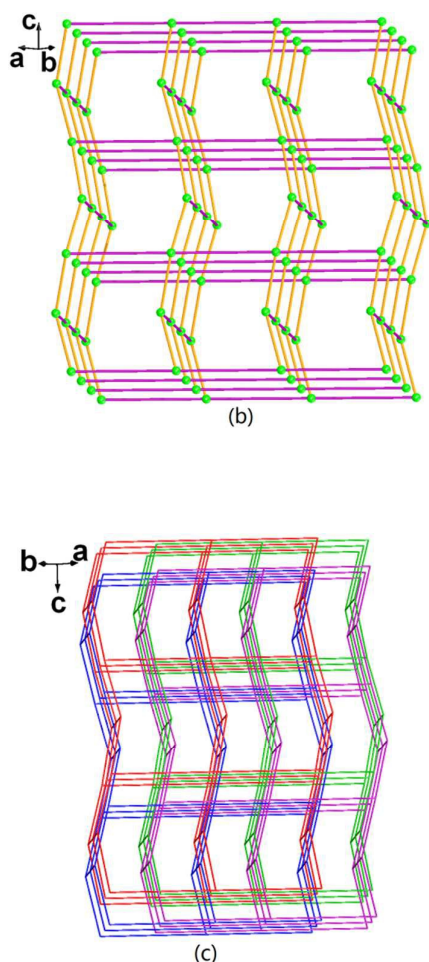


Fig. 3 (a) View of the 3D network of **1**. (b) Schematic view of a (6⁵-8) topological net of **1**. The cyan balls represent 4-connecting Zn centre. Each violet and orange line represents one bimpa and one 5-Me-1,3-BDC ligands. (c) View of 4-fold interpenetrating mode of **1**.

For **2**, two 1D chains are interconnected through bimpa ligands to form 1D tube (Fig. 4a). Such 1D tubes are parallelly interpenetrated to generate a 2D overall entanglement (Fig. 4b), which are further connected by hydrogen-bonding interactions (N3-H3A...O13ⁱ; O13-H13B...O3; O13-H13A...O8) (Table S2) and the π ... π stacking interactions between phenyl rings of bimpa ligands (centroid-to-centroid distances of 4.300 Å) to afford a 3D supramolecular structure (Fig. 4c).

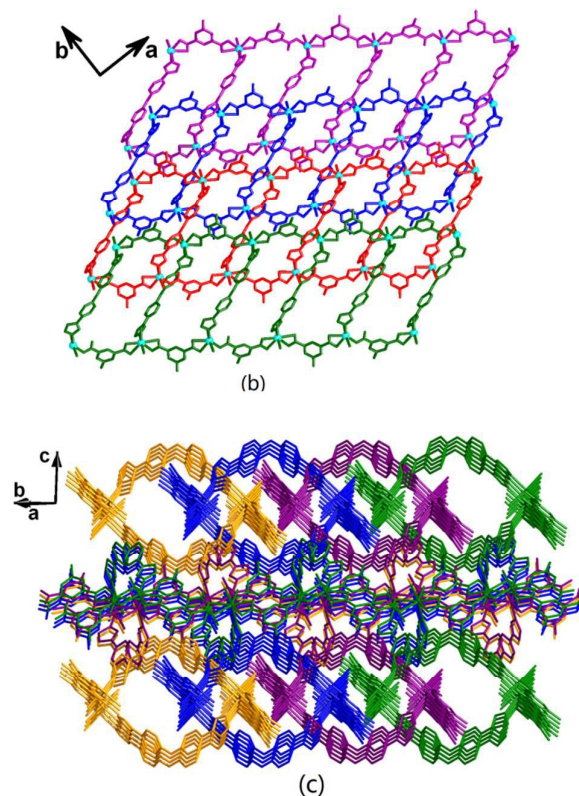
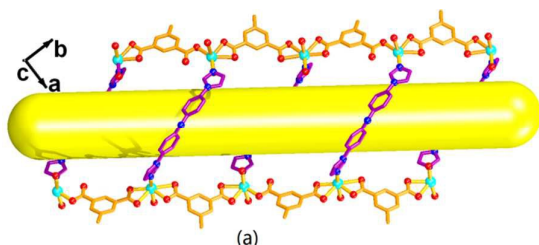


Fig. 4 (a) View of the 1D tube of **2** looking down the *c* axis. (b) View of 2-fold interpenetrating mode of **2** looking down the *c* axis (c) View of 3D supermolecular frameworks of **2**.

For **3** and **4**, bimpa ligands further link their respective 1D chains, resulting in two different 2D layers, such as a (6⁵-8) net *via* bimpa ligands in a criss-cross fashion (**3**) (Fig. 5a) and a 2D net consisted of 1D elliptical channels (**4**) (Fig. 5c). Moreover, these layers are connected by weak hydrogen-bonding interactions (Table S2) and intermolecular π ... π interactions between bimpa molecules in different layers to result in a 3D supermolecular structure (5b and 5d). Upon removal of guest molecules, the effective free volumes of **1-4** calculated by PLATON analysis are 6.3 % per unit cell volume (317.2 Å³ of the 4998.0 Å³ unit cell volume) (**1**), 3.8 % per unit cell volume (151.7 Å³ of the 3958.5 Å³ unit cell volume) (**2**), 3.8 % per unit cell volume (112.2 Å³ of the 2938.1 Å³ unit cell volume) (**3**) and 11.6 % per unit cell volume (350.0 Å³ of the 3024.0 Å³ unit cell volume) (**4**).

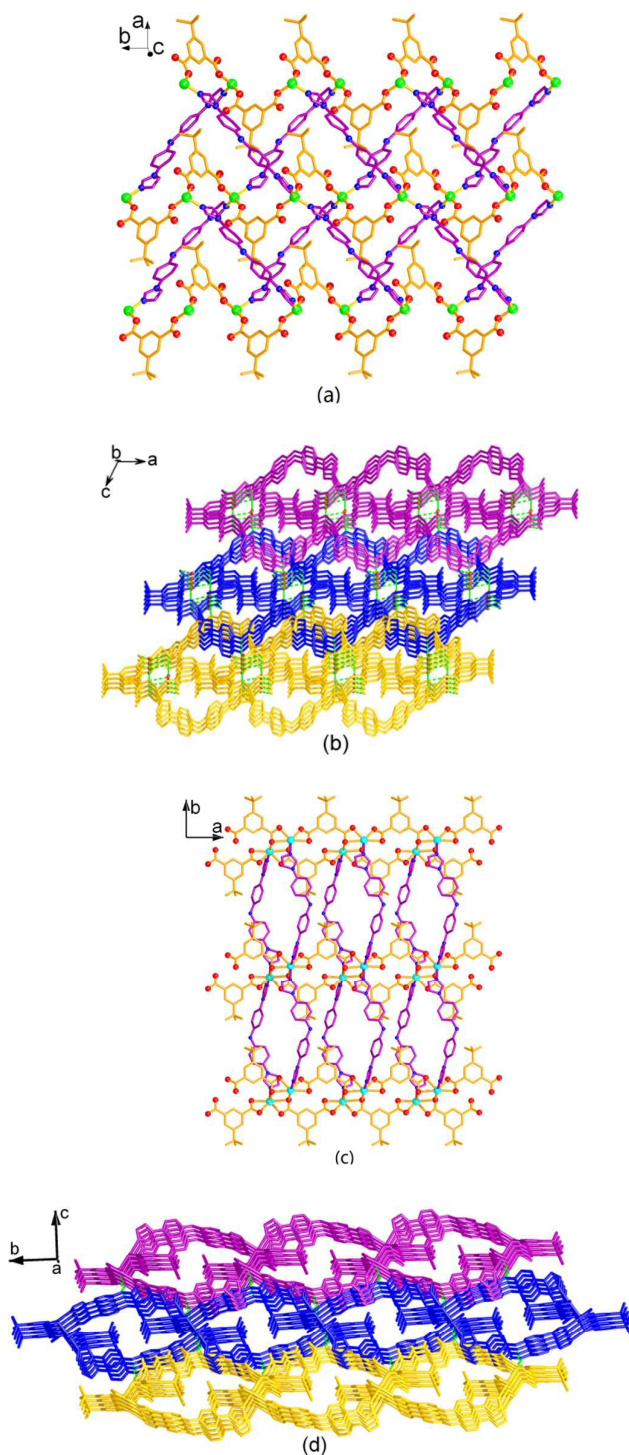


Fig. 5 (a) View of the 2D network of **3** in a criss-cross fashion extending along the *ab* plane. (b) View of 3D supermolecular frameworks of **3** (looking down the *b* axis). The red, green and cyan balls represent O, Zn and Cd atoms. (c) View of the 2D network of **4** extending along the *ab* plane. (d) View of 3D supermolecular frameworks of **4** (looking down the *a* axis).

As typical N-donor bidentate ligands, bi-imidazolyl ligands have been widely used to construct metal-organic coordination architectures with aromatic dicarboxylic acids. The previously prepared complexes $[\text{Cd}(5\text{-Me-1,3-}$

$\text{BDC})(\text{bimb})]_n$ ($\text{bimb} = 4,4'$ -bis(1-imidazolyl)biphenylene) were constructed from a linear *bimb* showing a pillared-layer structure.^{12a} When we introduced a bent *bimpa* ligand, a 4-fold interpenetrating 3D framework $[\text{Zn}_2(5\text{-Me-1,3-BDC})_2(\text{bimpa})_2]_n$ (**1**), a 3D supramolecular architecture based on 2D entanglements $\{[\text{Cd}_2(5\text{-Me-1,3-BDC})_2(\text{bimpa})(\text{H}_2\text{O})_4] \cdot \text{H}_2\text{O}\}_n$ (**2**) were produced. When 5-*tb*-1,3- H_2BDC with large-sized 5-*tert*-butyl group instead of 5-Me-1,3- H_2BDC , we obtained two 3D supramolecular architectures based on 2D layers $[\text{Zn}(5\text{-tb-1,3-BDC})(\text{bimpa})] \cdot 2\text{H}_2\text{O}\}_n$ (**3**) and $\{[\text{Cd}(5\text{-tb-1,3-BDC})(\text{bimpa})] \cdot \text{H}_2\text{O}\}_n$ (**4**). Thus, although the coordination sites of *bimb* and *bimpa* are very similar, their coordination geometry is obviously different presumably as a result of the different skeleton of the ligands. These structural diversity derived from the metal-bi(imidazolyl)/carboxylates systems give us the opportunity to systematically study their properties such as photoluminescence and photocatalytic activity.¹²

Thermal and photoluminescent properties

Thermogravimetric experiments were carried out to study the thermal stability of **1–4** (Fig. S8). The thermogravimetric analyses revealed that **1–4** were stable up to 301 °C (**1**), 414 °C (**2**), 300 °C (**3**) and 352 °C (**4**). For **1**, only one weight loss of 84.90% from 301 °C to 798 °C (**1**) amounts roughly to the loss of *bimpa* and 5-Me-1,3-BDC ligands (calculated 85.33%). For **2**, the first weight loss of 8.30% from 40 °C to 106 °C corresponds roughly to the loss of one uncoordinated water molecules and four coordinated water molecules per formula unit (calculated 9.26%). The second weight loss of 65.48% from 414 °C to 790 °C approximately amounts to the loss of all *bimpa* and 5-Me-1,3-BDC (calculated 64.34%). For **3**, the first weight loss of 4.75% from 40 °C to 80 °C corresponds roughly to the loss of two uncoordinated water molecules (calculated 5.79%). The second weight loss of 82.19% from 283 °C to 795 °C approximately amounts to the loss of all *bimpa* and 5-*tb*-1,3-BDC (calculated 81.38%). For **4**, the first weight loss of 3.20% from 40 °C to 95 °C corresponds roughly to the loss of one uncoordinated water molecules per formula unit (calculated 2.74%). The second weight loss of 78.66% from 352 °C to 780 °C approximately amounts to the loss of all *bimpa* and 5-*tb*-1,3-BDC (calculated 77.56%). In all cases, the decomposition residue species, according to X-ray fluorescence analysis, was assumed to be ZnO (15.10% vs calculated 14.67% (**1**) and 15.06% vs calculated 12.83% (**3**)) or CdO (26.22% vs calculated 26.40% (**2**), 19.24% vs calculated 19.70% (**4**)).

The photoluminescent properties of **1–4** in the solid state were investigated at ambient temperature (Fig. 6). For **1**, upon excitation at 307 nm (**1**), it exhibited photoluminescence with emission maxima at 370 and 383 nm, which were blue-shifted compared to that of the ligand *bimpa* ($\lambda_{\text{em}} = 405$ nm, $\lambda_{\text{ex}} = 345$ nm). The emission of **1** may be tentatively assigned to be the π - π^* intraligand fluorescence and ligand-to-ligand charge transfer (LLCT).^{5b} For **2, 3** and **4**, upon excitation at 375 nm (**2**), 305 nm (**3**) and 263 nm (**4**), they exhibited photoluminescence with emission maxima at 469 nm (**2**), 423 nm (**3**) and 417 nm (**2**) respectively. It is noted that the emission maxima of **2, 3**

and **4**, are red-shifted compared to that of bimpa. The bands might be assigned as the metal-to-ligand charge transfer (MLCT) with electrons being transferred from the Zn(II) or Cd(II) centres to the unoccupied p* orbitals of the imidazolyl groups of bimpa, according to the literature.¹⁹

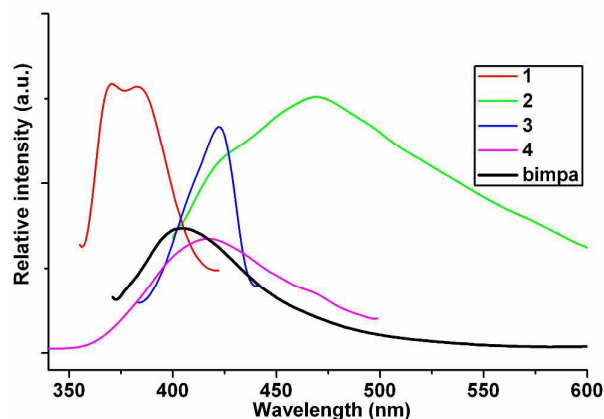


Fig. 6 The emission spectra of **1**, **2**, **3**, **4** and bimpa in solid state at ambient temperature.

Solid-state diffuse-reflection study

The UV-vis absorption spectra of **1-4** in the solid-state displayed in Fig S2. The electronic spectra of **1-4** show bands with maxima at ca. 318, 316, 324 and 320 nm. The absorption (α/S) data were calculated from the reflectance using the Kubelka-Munk function²⁰:

$$\alpha/S = \frac{(1 - R)^2}{2R}$$

Where α is the absorption, S is the scattering coefficient, and R is the reflectance at a given energy. The energy band gaps (Eonset) obtained by extrapolation of the linear portion of the absorption edges were estimated to be 3.09 eV (**1**), 3.17 eV (**2**), 2.95 eV (**3**), and 2.86 eV (**4**) (Figure 7). These wide band gap indicated that **1-4** may possess the potential capacity for semiconductor materials such as photocatalytic reaction.²¹

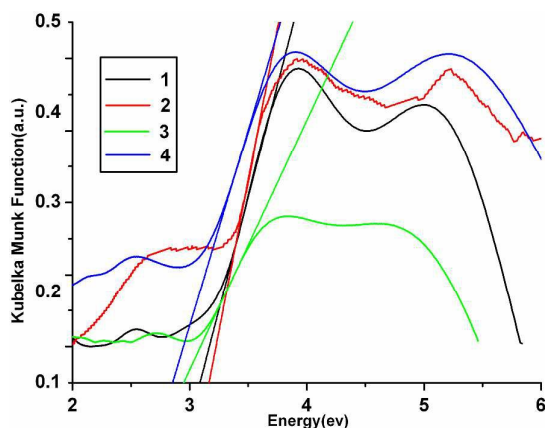
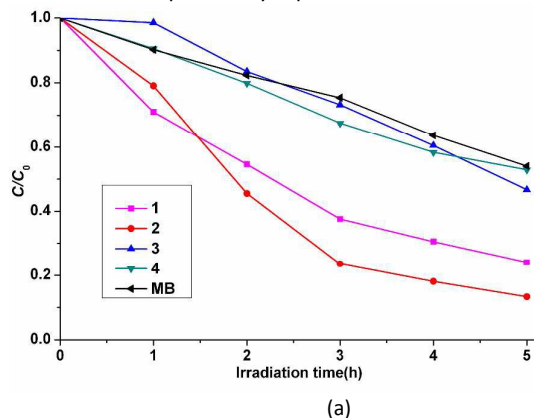
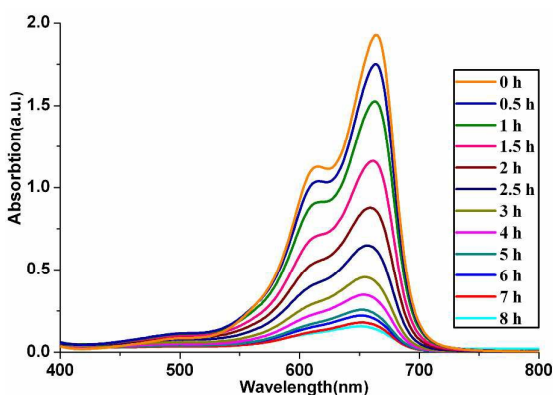


Fig. 7 Solid-state optical diffuse-reflection spectra of **1-4** derived from diffuse reflectance data at ambient temperature.

Photocatalytic Properties

Recently, many CPs have been employed as effective photocatalytic materials to decompose organic dyes into less dangerous products.²² Methylene blue (MB), a widely used organic dye in textile industry, was selected to evaluate the photocatalytic activities of complexes **1-4** under UV irradiation. The degradation progress was monitored by observing the intensity of the characteristic absorption band of MB at 663 nm. We used a 300 W high pressure mercury vapor lamp with circulating water cooling system at 10 cm distance between the liquid surface and the lamp. When no catalyst was added, MB could be degraded by ca. 45.9 % within 5 hours under UV irradiation, but the rate for decomposition became slow in the later time, which was consistent with those reported in the literature²³ (Fig. S3†). The concentrations of MO versus irradiation time of **1-4** were plotted in Fig.8a. After 5 h of UV irradiation, the degradation ratios are 75.9%, 86.7%, 53.3% and 47.1%, respectively. The degradation rate agrees with **2** > **1** > **3** > **4**, which is perfectly consistent with the theoretical result.²⁴ For the low photocatalytic activity of complexes **3** and **4** (Fig. S6†), there may be several possible reasons such as the capture capability for MB, electronic charges on their solid surface, *et al.*²⁵ Studies on this respect are being investigated in our laboratory. Compared with **1**, **3** and **4** (Fig. S4-6), **2** showed a higher photoactivity and ca. 91.7 % of MB was degraded in about 8 h under UV light irradiation (Fig. 8b), which means the long reaction time do not effectively increase the photodegradation rate at the later reaction stage. The proposed photocatalytic degradation mechanism was very similar to those previously reported²⁵.





(b)

Fig. 8 (a) Comparison of the catalytic activity of **1-4** and without catalyst in the photodegradation of MB under UV light irradiation. (b) UV-Vis absorption spectra of the MB solutions degraded by **2** under UV irradiation at different time intervals.

In addition, the photostability of complexes **1-4** was monitored by PXRD analysis during the course of the photocatalytic reactions. The PXRD confirmed that complexes **1-4** can be recovered from the catalytic system and reused without obvious loss of crystallinity as revealed by PXRD analysis (Fig. S1†). These results imply that complex **2** can be robust catalysts for MB photodegradation.

Conclusions

In summary, an assembly bis-(4-imidazol-1-yl-phenyl)-amine (bimpa) with Zn(II) or Cd(II) salt and 5-methyl-1,3-benzenedicarboxylic acid (5-Me-1,3-H₂BDC) or 5-tert-butyl-1,3-benzenedicarboxylic acid (5-tb-1,3-H₂BDC), results in the formation of four coordination polymers with diverse networks, which attribute to the coordination requirement of the metal ions and steric effects of alkyl groups. The photoluminescent and optical properties of **1-4** were also examined. Furthermore, the photocatalytic activities of **1-4** were evaluated by the decomposition of methylene blue in aqueous solution. It was found that the photocatalytic decomposition of MB catalyzed by **2** was faster than those initiated by **1, 3** and **4**. The better catalytic performance of **2** may be ascribed to properties of electronic charges on its solid surface. These results provided an interesting insight into the influence of metal ions or the substituent groups on the phenyl ring of 1,3-benzenedicarboxylic acid on the structures and properties of the final products.

Acknowledgments

The authors thanked the National Natural Science Foundation of China (No. 21201025), the NSF of Jiangsu Province (No. BK2012643, 12KJA150001), the Natural Science Foundation of the Education Committee of Jiangsu Province of China (No. 14KJA150001, 14KJB150001), the Scientific

Research Project of Changshu Institute of Technology (No. QT1313), the Start-up Grant from Changshu Institute of Technology (No. XZ1314). The authors are grateful to the useful comments of the reviewers and the editor.

References

- (a) T. R. Cook, Y. R. Zheng and P. J. Stang, *Chem. Rev.*, 2013, **113**, 734; (b) H. Furukawa, K. E. Cordova, M. O'Keeffe and O. M. Yaghi, *Science*, 2013, **341**, 974; (c) N. Stock and S. Biswas, *Chem. Rev.*, 2012, **112**, 933; (d) J. Q. Wang, C. X. Ren and G. X. Jin, *Organometallics*, 2006, **25**, 74.
- (a) P. Nugent, Y. Belmabkhout, S. D. Burd, A. J. Cairns, R. Luebke, K. Forrest, T. Pham, S. Ma, B. Space, L. Wojtas, M. Eddaoudi and M. J. Zaworotko, *Nature*, 2013, **495**, 80; (b) R. B. Lin, T. Y. Li, H. L. Zhou, C. T. He, J. P. Zhang and X. M. Chen, *Chem. Sci.*, 2015, **6**, 2516; (c) L. J. Murray, M. Dincă and J. R. Long, *Chem. Soc. Rev.*, 2009, **38**, 1294.
- (a) D. Liu, J. P. Lang and B. F. Abrahams, *J. Am. Chem. Soc.*, 2011, **133**, 11042; (b) J. R. Li, J. Sculley and H. C. Zhou, *Chem. Rev.*, 2012, **112**, 869; (c) J. Y. Cheng, P. Wang, J. P. Ma, Q. K. Liu and Y. B. Dong, *Chem. Commun.*, 2014, **50**, 13672; (d) T. A. Makal, J. R. Li, W. Lu and H. C. Zhou, *Chem. Soc. Rev.*, 2012, **41**, 7761; (e) Y. X. Tan, F. Wang, Y. Kang and J. Zhang, *Chem. Commun.*, 2011, **47**, 770.
- (a) M. Wriedt, A. A. Yakovenko, G. J. Haider, A. V. Prosvirin, K. R. Dunbar and H. C. Zhou, *J. Am. Chem. Soc.*, 2013, **135**, 4040; (b) D. Aulakh, J. B. Pyser, X. Zhang, A. A. Yakovenko, K. R. Dunbar and M. Wriedt, *J. Am. Chem. Soc.*, 2015, **137**, 9254; (c) M. Clemente-León, E. Coronado, C. Martí-Gastaldo and F. M. Romero, *Chem. Soc. Rev.*, 2011, **40**, 473; (d) F. Gao, L. Cui, Y. Song, Y. Z. Li, J. L. Zuo, *Inorg. Chem.*, 2014, **53**, 562.
- (a) S. S. Nagarkar, B. Joarder, A. K. Chaudhari, S. Mukherjee and S. K. Ghosh, *Angew. Chem. Int. Ed.*, 2013, **52**, 2881; (b) J. Cui, Y. F. Yue, G. D. Qian and B. L. Chen, *Chem. Rev.*, 2012, **112**, 1126; (c) J. Rocha, L. D. Carlos, F. A. A. Paz and D. Ananias, *Chem. Soc. Rev.*, 2011, **40**, 926; (d) Y. Li, S. S. Zhang and D. T. Song, *Angew. Chem. Int. Ed.*, 2013, **52**, 710; (e) J. H. Wang, M. Li and D. Li, *Chem. Sci.*, 2013, **4**, 1793; (f) X. P. Wang, T. P. Hu and D. Sun, *CrystEngComm*, 2015, **17**, 3393.
- (a) H. L. Jiang, T. A. Makal and H. C. Zhou, *Coord. Chem. Rev.*, 2013, **257**, 2232; (b) Q. L. Zhu, J. Li and Q. Xu, *J. Am. Chem. Soc.*, 2013, **135**, 10210; (c) M. Yoon, R. Srirambalaji and K. Kim, *Chem. Rev.*, 2012, **112**, 1196; (d) M. Zhao, S. Ou and C. D. Wu, *Acc. Chem. Res.*, 2014, **47**, 1199.
- (a) L. Luo, K. Chen, Q. Liu, Y. Lu, T. Okamura, G. C. Lv, Y. Zhao and W. Y. Sun, *Cryst. Growth Des.*, 2013, **13**, 2312; (b) J. J. Wang, T. L. Hu and X. H. Bu, *CrystEngComm*, 2011, **13**, 5152; (c) C. R. Murdock and D. M. Jenkins, *J. Am. Chem. Soc.*, 2014, **136**, 10983; (d) D. Sun, Z. H. Wei, C. F. Yang, D. F. Wang, N. Zhang, R. B. Huang and L. S. Zheng, *CrystEngComm*, 2011, **13**, 1591; (e) A. Hua, Y. Zhao, Y. S. Kang, Y. Lu and W. Y. Sun, *Dalton Trans.*, 2015, **44**, 11524; (f) X. L. Zhao and W. Y. Sun, *CrystEngComm*, 2014, **16**, 3247.
- (a) X. L. Wang, J. Luan, F. F. Sui, H. Y. Lin, G. C. Liu and C. Xu, *Cryst. Growth Des.*, 2013, **13**, 3561; (b) D. Zhao, D. J. Timmons, D. Q. Yuan and H. C. Zhou, *Acc. Chem.*

- Res., 2011, **44**, 123; (c) L. H. Cao, Y. L. Wei, Y. Yang, H. Xu, S. Q. Zang, H. W. Hou and T. C. W. Mak, *Cryst. Growth Des.*, 2014, **14**, 1827; (d) W. G. Lu, D. C. Zhong, L. Jiang and T. B. Lu, *Cryst. Growth Des.*, 2012, **12**, 3675; (e) H. R. Fu, Z. X. Xu, and J. Zhang, *Chem. Mater.*, 2015, **27**, 205.
- 9 (a) M. Du, C. P. Li, C. S. Liu and S. M. Fang, *Coord. Chem. Rev.*, 2013, **257**, 1282; (b) B. Y. Li, Y. M. Zhang, D. X. Ma, T. L. Ma, Z. Shi and S. Q. Ma, *J. Am. Chem. Soc.*, 2014, **136**, 1202; (c) F. L. Thorp-Greenwood, T. K. Ronson and M. J. Hardie, *Chem. Sci.*, 2015, **6**, 5779.
- 10 L. F. Ma, L. Y. Wang, J. L. Hu, Y. Y. Wang and G. P. Yang, *Cryst. Growth Des.*, 2014, **14**, 240.
- 11 (a) C. T. He, L. Jiang, Z. M. Ye, R. Krishna, Z. S. Zhong, P. Q. Liao, J. Q. Xu, G. F. Ouyang, J. P. Zhang and X. M. Chen, *J. Am. Chem. Soc.*, 2015, **137**, 7217; (b) J. M. Yu and P. B. Balbuena, *ACS Sustainable Chem. Eng.*, 2015, **3**, 117; (c) D. Y. Ma, Y. W. Li and Z. Li, *Chem. Commun.*, 2011, **47**, 7377; (d) G. K. H. Shimizu, R. Vaidhyanathan and J. M. Taylor, *Chem. Soc. Rev.*, 2009, **38**, 1430.
- 12 (a) H. J. Cheng, H. X. Li, Z. G. Ren, C. N. Lü, J. Shi and J. P. Lang, *CrystEngComm*, 2012, **14**, 6064; (b) J. Xu, X. Q. Yao, L. F. Huang, Y. Z. Li and H. G. Zheng, *CrystEngComm*, 2011, **13**, 857; (c) L. L. Wen, J. B. Zhao, K. L. Lü, Y. H. Wu, K. J. Deng, X. K. Leng, D. F. Li, *Cryst. Growth Des.*, 2012, **12**, 1603; (d) L. L. Wen, L. Zhou, B. G. Zhang, X. G. Meng, H. Qu and D. F. Li, *J. Mater. Chem.*, 2012, **22**, 22603; (e) Y. X. Sun and W. Y. Sun, *CrystEngComm*, 2015, **17**, 4045.
- 13 H. J. Cheng, M. Yu, H. X. Li, C. N. Lü, D. X. Li, M. M. Chen, Z. G. Ren and J. P. Lang, *J. Coord. Chem.*, 2013, **66**, 2335.
- 14 H. J. Cheng, R. X. Yuan, C. N. Lü and J. P. Lang, *Inorg. Chem. Commun.*, 2014, **40**, 138.
- 15 V. Polshettiwar, R. S. Varma, *Acc. Chem. Res.*, 2008, **41**, 629.
- 16 B. E. Love, and E. G. Jones, *Synth. Commun.*, 1999, **29**, 2831.
- 17 (a) G. M. Sheldrick, SHELXS-97, *Program for Solution of Crystal Structures*, University of Göttingen, Germany, 1997; (b) G. M. Sheldrick, SHELXL-97, *Program for Refinement of Crystal Structures*, University of Göttingen, Germany, 1997.
- 18 C. N. Lü, M. M. Chen, W. H. Zhang, D. X. Li, M. Dai and J. P. Lang, *CrystEngComm*, 2015, **17**, 1935.
- 19 D. Liu, H. X. Li, L. L. Liu, H. M. Wang, N. Y. Li, Z. G. Ren and J. P. Lang, *CrystEngComm*, 2010, **12**, 3708.
- 20 (a) W. W. Wendlandt and H. G. Hecht, *Reflectance Spectroscopy*, Interscience Publishers, New York, 1966; (b) W. W. Xiong, E. U. Athersh, Y. T. Ng, J. F. Ding, T. Wu and Q. C. Zhang, *J. Am. Chem. Soc.*, 2013, **135**, 1256.
- 21 (a) C. G. Silva, A. Corma and H. García, *J. Mater. Chem.*, 2010, **20**, 3141; (b) S. B. Wang and X. C. Wang, *Small*, 2015, **11**, 3097.
- 22 (a) X. Y. Wu, H. X. Qi, J. J. Ning, J. F. Wang, Z. G. Ren and J. P. Lang, *Applied Cat. B Environ.*, 2015, **168**, 98; (b) T. Zhang and W. B. Lin, *Chem. Soc. Rev.*, 2014, **43**, 5982; (c) J. Zhao, W. W. Dong, Y. P. Wu, Y. N. Wang, C. Wang, D. S. Li and Q. C. Zhang, *J. Mater. Chem. A*, 2015, **3**, 6962; (d) X. Lang, X. Chen and J. Zhao, *Chem. Soc. Rev.*, 2014, **43**, 473. (e) R. Li, X. Q. Ren, H. W. Ma, X. Feng, Z. G. Lin, X. G. Li, C. W. Hu and B. Wang, *J. Mater. Chem. A*, 2014, **2**, 5724; (f) Y. L. Hou, R. W. Y. Sun, X. P. Zhou, J. H. Wang and D. Li, *Chem. Commun.*, 2014, **50**, 2295; (g) M. Alvaro, E. Carbonell, B. Ferrer, F. X. L. i Xamena and H. Garcia, *Chem. Eur. J.*, 2007, **13**, 5106; (h) M. A. Nasalevich, M. van der Veen, F. Kapteijn and J. Gascon, *CrystEngComm*, 2014, **16**, 4919; (i) T. Wen, D. X. Zhang, J. Liu, R. Lin and J. Zhang, *Chem. Commun.*, 2013, **49**, 5660.
- 23 (a) H. R. Fu, Y. Kang, and J. Zhang, *Inorg. Chem.*, 2014, **53**, 4209; (b) S. M. Chen, Y. F. Chen, R. Lin, X. P. Lei and J. Zhang, *CrystEngComm*, 2013, **15**, 10423.
- 24 M. Dai, X. R. Su, X. Wang, B. Wu, Z. G. Ren, X. Zhou and J. P. Lang, *Cryst. Growth Des.*, 2014, **14**, 240.
- 25 (a) C. C. Wang, J. R. Li, X. L. Lv, Y. Q. Zhang, G. S. Guo, *Energy Environ. Sci.*, 2014, **7**, 2831; (b) C. C. Chen, W. H. Ma and J. C. Zhao, *Chem. Soc. Rev.*, 2010, **39**, 4206.

Graphic Contents Entry

Four new coordination polymers have been solvothermally synthesized to explore their diverse networks and photocatalytic properties.

